



Hydrothermal syntheses, structures and characterizations of two luminescent cadmium(II) complexes with *p*-xylenediphosphonic acid and N-donor ligands

Yan-Qiong Sun*, Jin Hu, Han-Hui Zhang, Yi-Ping Chen

Department of Chemistry, Fuzhou University, Fuzhou 350002, People's Republic of China

ARTICLE INFO

Article history:

Received 31 August 2011

Received in revised form

14 November 2011

Accepted 28 November 2011

Available online 8 December 2011

Keywords:

Hydrothermal synthesis

Cadmium diphosphonate

Structure

Second ligand

ABSTRACT

Two novel cadmium diphosphonates $[\text{Cd}(\text{cis-H}_4\text{BDPP})(2,2'\text{-bipy})_2] \cdot (\text{trans-H}_2\text{BDPP})_n$ (**1**) and $[\text{Cd}(\text{trans-H}_2\text{BDPP})(\text{phen})]_n$ (**2**) ($\text{H}_4\text{BDPP} = p\text{-xylenediphosphonic acid}$, $\text{phen} = 1,10\text{-phenanthroline}$, $2,2'\text{-bipy} = 2,2'\text{-bipyridine}$) were hydrothermally synthesized from *p*-xylenediphosphonic acid and $\text{CdSO}_4 \cdot 3\text{H}_2\text{O}$ with phen or 2,2'-bipy as second ligand components and characterized by means of elemental analyses, IR, TG analysis, luminescence spectroscopy and single crystal X-ray diffraction. Compound **1** consists of a novel one-dimensional (1D) sinusoidal $[\text{Cd}(\text{cis-H}_4\text{BDPP})(2,2'\text{-bipy})_2]$ chains and *trans*- H_2BDPP anions. Compound **2** possesses a three-dimensional architecture built from double zigzag $-\text{Cd}-\text{O}-\text{P}-\text{O}-\text{Cd}-$ chains pillared by *trans*-*p*-xylylenediphosphonate ligands from four different directions. There are hexagonal channels running along the *c*-axis and the coordinated phen ligands suspend in the hexagonal channels. The results indicate that *p*-xylenediphosphonic acid can adopt varied coordination modes and conformations in the formation of the complexes and the influence of the N-donor ligands on the structure of the complexes is discussed.

© 2011 Elsevier Inc. All rights reserved.

1. Introduction

As a novel inorganic–organic hybrid material, metal organic phosphonates/di phosphonates have attracted more and more inorganic and material chemists' attention due to their abundant framework styles, well thermal and chemical stability [1], and their potential applications in the areas of catalysis, ion exchange, proton conductivity, intercalation chemistry, photochemistry and materials chemistry [2]. In order to design metal phosphonates with additional functionality, a variety of functional groups such as amino acids, crown ethers, amino groups and carboxylates have been attached to the phosphonate groups [3–5]. The use of multifunctional phosphonic acids in the synthesis of metal phosphonates may not only result in new structure types of metal phosphonates, but also bring interesting properties [6–7]. Furthermore, many research activities have concerned the synthesis of hybrid frameworks by incorporating a second organic ligand such as oxalate, carboxylic acid, sulfonic acids, 2,2'-bipyridine, 4,4'-bipyridine, or 1,10-phenanthroline into the structures of metal phosphonates recently [8–11]. That is because these molecules can act as pillars between neighboring layers or be grafted into the inorganic layer to form new hybrid architectures.

p-Xylenediphosphonic acid, as a multidentate ligand, has been used by us and other groups in the construction of metal-organic frameworks with both transition metal (TM) and lanthanide (Ln) ions as nodes [12–17]. However, the incorporation of second ligand into metal *p*-xylenediphosphonate frameworks is rare [18]. We chose *p*-xylenediphosphonic acid as the organic bridging linker, based on the following considerations: (a) it has four protonated hydrogens and can be successively deprotonated to generate H_3BDPP^- , $\text{H}_2\text{BDPP}^{2-}$, HBDPP^{3-} , BDPP^{4-} dependent on the pH level, and hence may supply four different valence anions as compensating charge and various, acidity-dependent coordination modes; (b) *p*-Xylylenediphosphonic acid is a good example of flexible ditopic ligand in which $(-\text{CH}_2-\text{P}-)$ bond can adopt *cis/trans* conformation with respect to benzene ring. The flexibility of ligand provides a high likelihood for generation of fascinating structures. The final structures based on flexible ligands are prone to several synthetic conditions. It is also important to note that rotations along single bond leads to the loss of control in designing. These factors make the synthesis of coordination polymers based on such flexible ligand a challenging task.

Here, we report two novel cadmium(II)-*p*-xylenediphosphonates with different auxiliary ligands, namely, $[\text{Cd}(\text{cis-H}_4\text{BDPP})(2,2'\text{-bipy})_2] \cdot (\text{trans-H}_2\text{BDPP})$ (**1**) and $\text{Cd}(\text{trans-H}_2\text{BDPP})(\text{phen})$ (**2**), respectively, which is the first example of incorporation of second ligand into cadmium(II)-*p*-xylenediphosphonates. In compound **1**, the 2,2'-bipy ligand as second ligand is introduced into cadmium(II)-*p*-xylenediphosphonate. The neutral ligands H_4BDPP in *cis* conformation

* Corresponding author. Fax: +86 591 22866340.
E-mail address: sunyq@fzu.edu.cn (Y.-Q. Sun).

bridge the Cd^{2+} to generate a 1D sinusoidal chain, which is stabilized by the deprotonated anion H_2BDPP in *trans* conformation. On the other hand, by using phen ligand as secondary ligand, the deprotonated anion $\text{H}_2\text{BDPP}^{2-}$ in *trans* conformation acts as the linker via its coordination to the Cd^{2+} resulting in a 3D architecture.

2. Experimental

2.1. Materials and physical measurements

All analytical reagent grade chemicals were commercially purchased and used without purification. The elemental analyses of C, H and N were performed with an Elementar Vario EL III elemental analyzer. The IR spectra were recorded with a Perkin-Elmer Spectrum 2000 FT-IR spectrometer in the range of 400–4000 cm^{-1} using the KBr pellet technique. Thermogravimetric (TG) analyses were conducted on a Perkin-Elmer TGA7 Thermal analyzer in an N_2 atmosphere with a heating rate of 10 $^\circ\text{C}/\text{min}$ from 25 $^\circ\text{C}$ to 800 $^\circ\text{C}$. The fluorescent spectra were recorded on an Edinburgh Instrument FL/FS-920 fluorescent spectrometer using Xe lamp for steady fluorescent and H_2 nanosecond flash lamp for transient fluorescence. The X-ray powder diffraction pattern was collected on a Panalytic X'pertPro diffractometer using $\text{CoK}\alpha$ radiation ($\lambda = 1.790 \text{ \AA}$).

2.2. Synthesis of H_4BDPP

The H_4BDPP was synthesized by a classical Arbuzov reaction followed by acidic hydrolysis of the ester of diphosphonic acid [19].

2.3. Synthesis of $[\text{Cd}(\text{H}_4\text{BDPP})(2,2'\text{-bipy})_2] \cdot (\text{H}_2\text{BDPP})$ (**1**)

H_4BDPP (0.07 g, 0.25 mmol), 2,2'-bipy (0.10 g, 0.5 mmol) were mixed with $\text{CdSO}_4 \cdot 3 \text{H}_2\text{O}$ (0.13 g, 0.5 mmol) in 5 mL of deionized distilled water, after reaction mixture was stirred to homogeneity, add NaF (0.01 g, 0.24 mmol) to the mixture and stirred homogeneity again. Then the mixture was sealed in a Teflon-lined stainless autoclave (15 mL) and heated at 160 $^\circ\text{C}$ for 3 day under autogenous pressure and then cooled to room temperature unaffectedly. The X-ray-diffraction-quality single colorless rod-like crystals **1** were collected in about 40% yield (based on Cd). Anal. Calcd for $\text{C}_{18}\text{H}_{19}\text{Cd}_{0.50}\text{N}_2\text{O}_6\text{P}_2$ ($M_r = 477.49$): C, 45.28%; H, 4.01%; N, 5.87%. Found: C, 45.15%; H, 3.86%; N, 5.74%. IR (cm^{-1}): 3444(m), 2704(w), 2331(w), 1595(m), 1505(m), 1472(m), 1440(m), 1257(s), 929(s), 847(s), 780(s), 731(m), 571(s), 510(s) (Fig. S1(a) in the supporting information).

2.4. Synthesis of $\text{Cd}(\text{H}_2\text{BDPP})(\text{phen})$ (**2**)

H_4BDPP (0.13 g, 0.5 mmol), Phen (0.10 g, 0.5 mmol) were mixed with $\text{CdSO}_4 \cdot 3 \text{H}_2\text{O}$ (0.26 g, 1.0 mmol) in 10 mL of deionized distilled water, after reaction mixture was stirred to homogeneity, add NaF (0.04 g, 1.0 mmol) to the mixture and stirred homogeneity again. Then the mixture was sealed in a Teflon-lined stainless autoclave (30 mL) and heated at 160 $^\circ\text{C}$ for 3 day under autogenous pressure and then cooled to room temperature unaffectedly. The X-ray-diffraction quality single colorless rod-like crystals **2** were collected in about 18% yield (based on Cd). Anal. Calcd for $\text{C}_{20}\text{H}_{18}\text{CdN}_2\text{O}_6\text{P}_2$ ($M_r = 556.70$): C, 43.15%; H, 3.26%; N, 5.03%. Found: C, 42.91%; H, 3.09%; N, 4.97%. IR (cm^{-1}): 3503(m), 3409(m), 2916(w), 2852(w), 2327(w), 1621(w), 1592(s), 1514(s), 1430(s), 1255(s), 930(s), 860(m), 792(s), 721(s), 556(s), 459(s) (Fig. S1(b)).

2.5. Crystal structure determination

The single-crystal X-ray diffraction measurement was carried out on a Rigaku Saturn 724 CCD area detector. Intensity data were

collected by a graphite-monochromatized $\text{MoK}\alpha$ radiation ($\lambda = 0.71073 \text{ \AA}$) using a ω scan mode at 298(2) K. The data sets were corrected for absorption by multi-scan technique. The structure was solved by direct methods and refined by full-matrix least-squares fitting on F^2 for observed reflections with $I > 2\sigma(I)$ with SHELXTL-97 [20]. All non-hydrogen atoms were refined with anisotropic thermal parameters. Hydrogen atoms attached to C were located at the geometrically calculated positions and refined with isotropic thermal parameters, while that attached to O of phosphonate group was added by difference Fourier maps and refined isotropically with $U_{\text{iso}}(\text{H}) = 1.5U_{\text{eq}}(\text{O})$. Further details of the crystallographic data and structure refinement for both are tabulated in Table 1. Selected bond lengths are listed in Tables 2 and 3.

Table 1
Crystal data and structure refinement for **1** and **2**.

| Compound | 1 | 2 |
|--|--|--|
| Empirical formula | $\text{C}_{18}\text{H}_{19}\text{Cd}_{0.50}\text{N}_2\text{O}_6\text{P}_2$ | $\text{C}_{20}\text{H}_{18}\text{CdN}_2\text{O}_6\text{P}_2$ |
| fw | 477.49 | 556.71 |
| Crystal system | Monoclinic | Monoclinic |
| Space group | $C2/c$ | $C2/c$ |
| <i>a</i> (Å) | 18.197(2) | 21.497(4) |
| <i>b</i> (Å) | 25.081(3) | 12.232(2) |
| <i>c</i> (Å) | 8.807(2) | 7.741(2) |
| α (deg.) | 90 | 90 |
| β (deg.) | 102.39(3) | 98.76(3) |
| γ (deg.) | 90 | 90 |
| <i>V</i> (Å ³) | 3925.9(1) | 2011.9(7) |
| <i>Z</i> | 8 | 4 |
| <i>D_c</i> (g cm ⁻³) | 1.616 | 1.838 |
| μ (mm ⁻¹) | 0.787 | 1.289 |
| <i>F</i> (000) | 1944 | 1112 |
| Unique data | 4495 [<i>R</i> (int)=0.0417] | 2285 [<i>R</i> (int)=0.0507] |
| Data with [<i>I</i> > 2 σ (<i>I</i>)] | 4249 | 2197 |
| GOF on F^2 | 1.052 | 1.013 |
| <i>R</i> ₁ ^a , <i>wR</i> ₂ ^b [<i>I</i> > 2 σ (<i>I</i>)] | 0.0523, 0.0877 | 0.0626, 0.1478 |
| <i>R</i> ₁ , <i>wR</i> ₂ (all data) | 0.0568, 0.0894 | 0.0654, 0.1496 |
| $\Delta\rho_{\text{max}}/\Delta\rho_{\text{min}}$ (e Å ⁻³) | 0.325/−0.333 | 0.873/−0.588 |

$$^a R_1 = \sum |F_o| - |F_c| / \sum |F_o|$$

$$^b wR_2 = \left[\sum [w(F_o^2 - F_c^2)]^2 / \sum [w(F_o^2)]^2 \right]^{1/2}$$

Table 2
Selected bond lengths (Å) for compounds **1** and **2**.

| Bond | Dist. | Bond | Dist. |
|--------------|----------|-----------|----------|
| 1 | | | |
| Cd(1)–O(1)#1 | 2.208(2) | P(1)–O(1) | 1.483(2) |
| Cd(1)–N(1) | 2.350(3) | P(1)–O(3) | 1.561(3) |
| Cd(1)–N(2) | 2.358(3) | P(1)–O(2) | 1.538(3) |
| P(2)–O(5) | 1.504(2) | P(2)–O(4) | 1.514(2) |
| P(2)–O(6) | 1.558(3) | | |
| 2 | | | |
| Cd(1)–O(2)#1 | 2.263(4) | P(1)–O(1) | 1.491(5) |
| Cd(1)–O(1) | 2.280(5) | P(1)–O(2) | 1.512(5) |
| Cd(1)–N(1) | 2.354(6) | P(1)–O(3) | 1.560(5) |

Symmetry transformations used to generate equivalent atoms: #1 $-x, y, -z + 1/2$.

Table 3
Parameters of hydrogen bonds for **1**.

| D–H | <i>d</i> (D–H) | <i>d</i> (H⋯A) | < DHA <i>d</i> (D⋯A) | A | Symmetry codes(\$) |
|------------|-------------------|-------------------|----------------------------|--------|------------------------------------|
| O(2)–H(20) | 0.86 | 1.62 | 174 | 2.4741 | O(6) |
| O(3)–H(30) | 0.85 | 1.72 | 170 | 2.5645 | O(4) |
| O(6)–H(60) | 0.85 | 1.79 | 164 | 2.6180 | O(4) _{\$} [x, −y, −1/2+z] |

3. Results and discussion

3.1. Structural description of $[\text{Cd}(\text{cis-H}_4\text{BDPP})(2,2'\text{-bipy})_2] \cdot (\text{trans-H}_2\text{BDPP})$ (**1**)

The X-ray crystal structure analysis reveals that compound **1** consists of 1D sinusoidal $[\text{Cd}(\text{cis-H}_4\text{BDPP})(2,2'\text{-bipy})_2]$ chains and $\text{trans-H}_2\text{BDPP}$ anions. The asymmetric unit contains one half of Cd^{2+} cation that resides on the twofold symmetry axis, one halves of $\text{cis-H}_4\text{BDPP}$ and $\text{trans-H}_2\text{BDPP}$ as well as two 2,2'-bipy ligands. As shown in the Fig. 1, the Cd^{2+} cation is six-coordinated by O atoms from two cis -xylenediphosphonic acids and four N atoms from two 2,2'-bipy. Its coordination geometry can be described as a slightly distorted octahedron. The bond lengths of $\text{Cd}(1)\text{-O}(1)$ is 2.208(2) Å, and for the $\text{Cd}(1)\text{-N}(1)$ and $\text{Cd}(1)\text{-N}(2)$ are 2.350(3) and 2.358(3) Å. These distances are comparable to those in other cadmium phosphonates [13].

In the compound **1**, it is interesting that there are two different conformations of p -xylenediphosphonic acid, cis - and trans -conformations (Fig. S2). The $\text{cis-H}_4\text{BDPP}$ is coordinated to the Cd centers with $\text{P}=\text{O}$ groups on both sides which is in good accordance with the $\text{P}-\text{O}$ bond distance of 1.481(7) Å, and thereby the charge is balanced by the uncoordinated phosphonic acid, $\text{trans-H}_2\text{BDPP}$ which is deprotonated from H_4BDPP to H_2BDPP . The existence of both cis and trans configurations in the same crystal structure is scarcely observed in metal p -xylenediphosphonates [18c]. Every $\text{cis-H}_4\text{BDPP}$, with a twofold axis passing through the center of aromatic ring, links two neighboring Cd^{2+} cations in one monodentate to form a one-dimensional (1D) sinusoidal chain running along c -axis. Two 2,2'-bipy fragments are attached to the 1-D chain as branches of the chain by coordinated Cd atoms at the same side in the same chain (Fig. 2(a)).

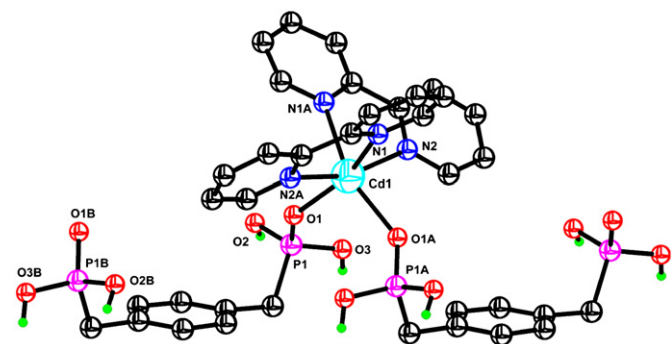


Fig. 1. Coordination environments of **1**, with thermal ellipsoids at 50% probability and partial atom numbering scheme, symmetry codes: A, $-x, y, 0.5-z$; B, $-x, y, -0.5-z$.

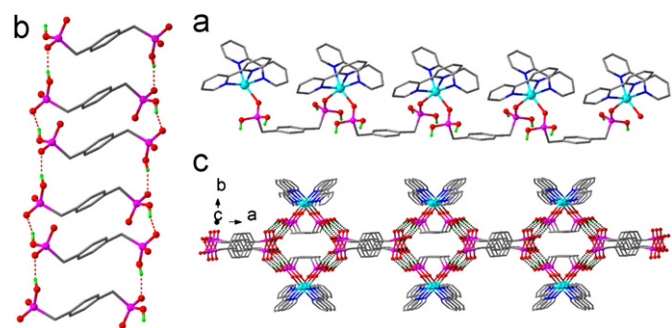


Fig. 2. (a) The one-dimensional (1D) sinusoidal chain bridged from $[\text{Cd}(2,2'\text{-bipy})_2]^{2+}$ units and $\text{cis-H}_4\text{BDPP}$ ligands in **1**. (b) The 1D ladder-like supra-molecular ribbon running along $[001]$ direction in **1**. (c) The 2-D supra-molecular tubular layer viewed along $[001]$ direction in **1**.

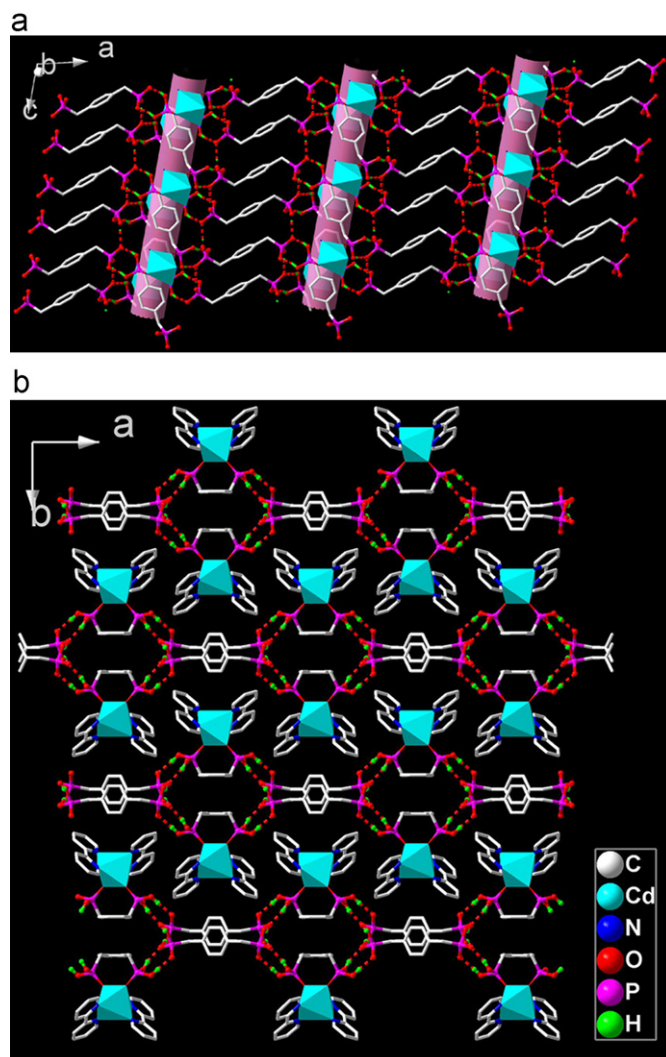


Fig. 3. (a) The 2-D supra-molecular tubular layer of **1** in the ac plane. (b) The packing structure of **1** viewed along $[001]$ direction.

Each $\text{cis-H}_4\text{BDPP}$ anion only acts as a donor of strong hydrogen bonds $\text{O}-\text{H}\cdots\text{O}$ with $\text{O}\cdots\text{O}$ distances of 2.47 and 2.56 Å, and each $\text{trans-H}_2\text{BDPP}$ acts as both acceptor and donor of bonds of the type $\text{O}-\text{H}\cdots\text{O}$ (Fig. S3). The $\text{trans-H}_2\text{BDPP}$ ligands are linked together by $\text{O}-\text{H}\cdots\text{O}$ hydrogen bonds to generate a 1D ladder-like ribbon (Fig. 2(b)). Two central-symmetry 1D sinusoidal chains are held together by $\text{O}-\text{H}\cdots\text{O}$ interactions between $\text{cis-H}_4\text{BDPP}$ and $\text{trans-H}_2\text{BDPP}$ ligands, thus yielding a tubular network (Fig. S4). The tubes are alternately connected, with the ribbons functioning as hinges. As result, a novel 2-D supra-molecular tubular layer is formed in the ac plane. The 2,2'-bipy ligands are above or below the layers (Figs. 2(c) and 3(a)). These 2D supra-molecular tubular layers stack in $-\text{ABAB}-$ modes along the b -axis (Fig. 3(b)).

3.2. Structural description of $\text{Cd}(\text{trans-H}_2\text{BDPP})(\text{phen})$ (**2**)

Compound **2** possesses a 3D architecture containing one-dimensional hexagonal channels along the c -axis. The Cd^{2+} cation, residing on the twofold symmetry axis, is six-coordinated and described as a distorted octahedron: two phen nitrogen ($\text{Cd}-\text{N}$: 2.354(6) Å), four phosphonate oxygen atoms from four $\text{trans-H}_2\text{BDPP}$ s ($\text{Cd}-\text{O}$: 2.263(4) and 2.280(5) Å) (Fig. 4). The H_2BDPP ligands in **2** adopts trans configuration, Each phosphonate group of $\text{trans-H}_2\text{BDPP}$ has two oxygens coordinated to Cd atoms

and one OH free groups, and each *trans*-H₂BDPP anions linked four Cd²⁺ ions in monodentate mode (Fig. S5).

Remarkably, there is a 1-D double zigzag inorganic chain constructed from corner-sharing Cd₂P₂ four-rings running along the *c*-axis (Figs. S6 and 5(a)). Two [CdO₄N₂] octahedra and two [PO₃C] tetrahedra are connected each other alternately to form the corner-sharing Cd₂P₂ four-rings (Fig. S6). Similar inorganic chains were observed in Zn[HO₃PCH₂(C₆H₄)CH₂PO₃H] [17] compound in which the 1-D linear inorganic chain consists of corner-sharing Zn₂P₂ four rings constructed from strictly alternating [ZnO₄] and [PO₃C] tetrahedra. The difference of these two inorganic chains lies in the coordination geometry of the metal atoms: Cd displaying six-coordinated octahedron and Zn showing four-coordinated tetrahedron. So in compound **2**, the inorganic chains are not linear but double zigzag. There are intermolecular hydrogen bonds O–H...O (O...O=2.647(7) Å) between the adjacent –PO₃H groups of the 1D zigzag chain which were not observed in Zn[HO₃PCH₂(C₆H₄)CH₂PO₃H] (Fig. S6). The inorganic chain links four other adjacent chains by –CH₂–C₆H₄–CH₂– groups along [110], [1–10], [–1–10] directions to form a 3D architecture (Fig. 5(b)). There are hexagonal channels running along the *c*-axis and with the dimensions of 8.44 × 13.99 Å in which the coordinated phen molecules protrude into the channels (Fig. 6). The hexagonal channels along the *c*-axis were not found in Zn[HO₃PCH₂(C₆H₄)CH₂PO₃H]. There are offset face-to-face π–π stacking interactions between the parallel 1,10-phen rings of the two inorganic chains along *b*-axis at a distance of 3.43 Å. The structure has 1D channels about 3.87 × 10.75 Å along the *b*-axis which also were observed in Zn[HO₃PCH₂(C₆H₄)CH₂PO₃H] (Fig. S7).

From the topological point of view, the 3-D framework of **2** is a 4-connected net. Because both Cd²⁺ cations and H₂BDPP ligands

act as four-connected node (Fig. 7) The overall is bimodal and adopts the PtS network topology with the point symbol of (4²·8⁴)₂. The extended point symbol is: (4·4·8₇·8₇·8₇·8₇)·(4·4·8₂·8₂·8₈·8₈). Tiling analysis showed that **2** contained two building blocks, tile [4²·8²] and tile [8⁴]. The intrinsic symmetry for tiling is P4₂/mmc with the transitivity [2232]. The structures of compound **2** and the reported Zn[HO₃PCH₂(C₆H₄)CH₂PO₃H] have the same topologies and different motifs. The difference lies in the second ligand 1,10-phen and the six-coordinated Cd atom.

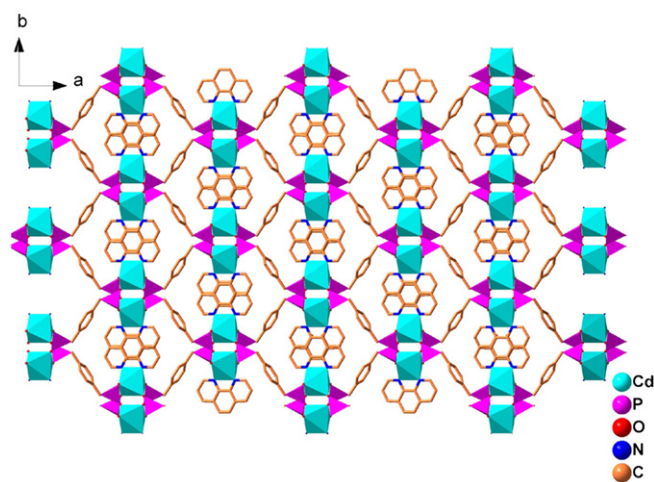


Fig. 6. The 3D framework viewed along the *c*-axis showing 1D nanoporous hexagonal channels.

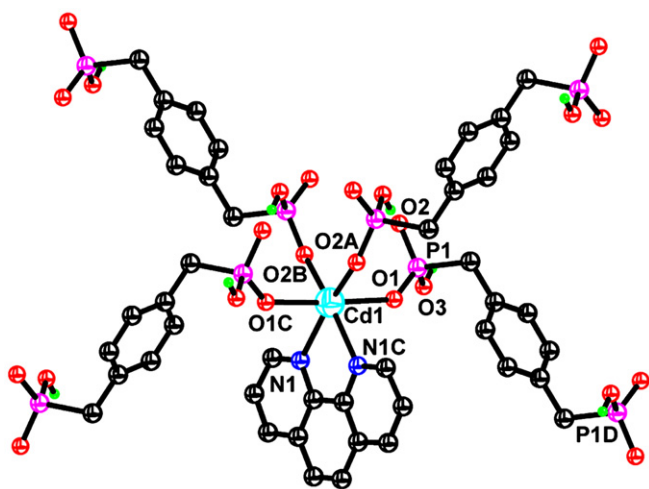


Fig. 4. Coordination environments of **2**, with thermal ellipsoids at 50% probability and partial atom numbering scheme, symmetry codes: A, *x*, 1–*y*, 0.5+*z*; B, 1–*x*, 1–*y*, –*z*; C, 1–*x*, *y*, 0.5–*z*; D, 1.5–*x*, 0.5–*y*, –*z*.

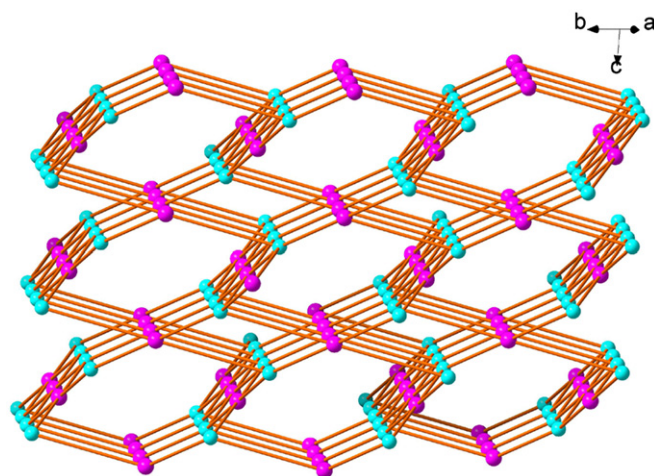


Fig. 7. PtS network topology of **1** with the point symbol of (4²·8⁴)₂. The 4-connected cyan nodes represent the Zn²⁺, while the 4-connected purple ones represent the H₂BDPP ligands.

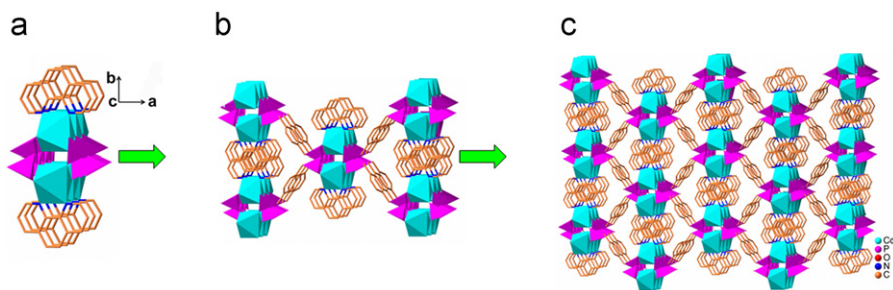


Fig. 5. (a) View of the 1D zigzag inorganic chain decorated by phen ligands along *c*-axis. (b) The construction of 3D framework through the inorganic chains linking other adjacent chains by –CH₂–C₆H₄–CH₂– groups of the ligands. (c) 3D framework viewed close along the *c*-axis.

3.3. Discussion

3.3.1. Influence of the second ligand

It is found that the second ligand plays an important role in this reaction and strongly affects the structure of the final products. For **1**, 2,2'-bipy was selected as a second ligand. All the cadmium ions form $[\text{Cd}(2,2'\text{-bpy})_2]^{2+}$ cations. The secondary ligand component blocks four coordination sites, i.e. three equatorial and one apical positions of cadmium octahedron, leaving one equatorial and one apical sites available for coordination with H_4BDPP . In order to meet this coordination requirement (i.e. to satisfy the coordination sites: one equatorial and one apical sites), a flexible non-rigid H_4BDPP ligand has to adopt a rare *cis* conformation and link two $[\text{Cd}(2,2'\text{-bpy})_2]^{2+}$ units to form 1D sinusoidal chain structure. This conformational freedom of H_4BDPP allows the existence of both *cis* and *trans* conformations in the same crystal structure. In **2**, the second ligand is a chelated ligand with large size, such as phen. Only one phen ligand chelated Cd atom to form $[\text{Cd}(1.10\text{-phen})]$, every $[\text{Cd}(1.10\text{-phen})]$ connects four *p*-xylenediphosphonate ligands from four different directions and each *p*-xylenediphosphonate ligand with *trans* configuration links four Cd atoms, generating a 3D architecture. The result implies that the subtle difference in auxiliary ligand has a great influence on the structure of the complexes.

3.3.2. Luminescent properties

The solid-state photoluminescent spectra for compound **1** and **2** were investigated at room temperature. H_4BDPP , 2,2'-bipy and phen display their characteristic emission peaks at 360 nm ($\lambda_{\text{ex}}=320$ nm), 496 nm ($\lambda_{\text{ex}}=495$ nm) and 381 nm ($\lambda_{\text{ex}}=339$ nm), respectively, which may be attributed to $\pi^* \rightarrow \pi$ transition of the ligands. For **1**, only one emission band appears with the maximum at 433 nm with lifetime of 3.156 ns upon excitation at 356 nm, which is red-shifted compared to that of the free H_4BDPP ligand (Fig. 8). As to the $4d^{10}$ valence electron configuration of the Cd(II) ion, the emission band of the Cd(II) complexes may be assigned to ligand-to-ligand charge transfer (LLCT), admixing with ligand-to-metal charge transfer (LMCT) as previously reported [21]. Compound **2** displays emission bands at 425 nm and 550 nm upon excitation at 350 nm (Fig. 9). The emission peak at 425 nm can probably be assigned to the intraligand ($\pi^* \rightarrow \pi$) fluorescent emission. The emission band at 550 nm may be attributed to ligand-to-metal charge transfer. The lifetime is 1.4137 ns for 425 nm emission peak and 3.874 ns for 550 nm emission band.

3.3.3. Thermal analysis

The thermal stability of **1** and **2** was examined by the TG analysis under dry air atmosphere from 40 to 700 °C. Compound **1** is stable up to 250 °C. The first weight loss of **1** is during 250 to

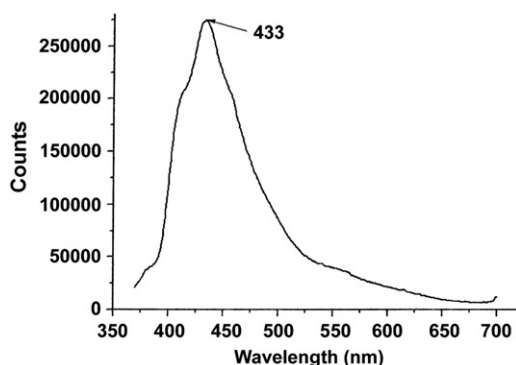


Fig. 8. Solid-state emission spectrum for compound **1** at room temperature.

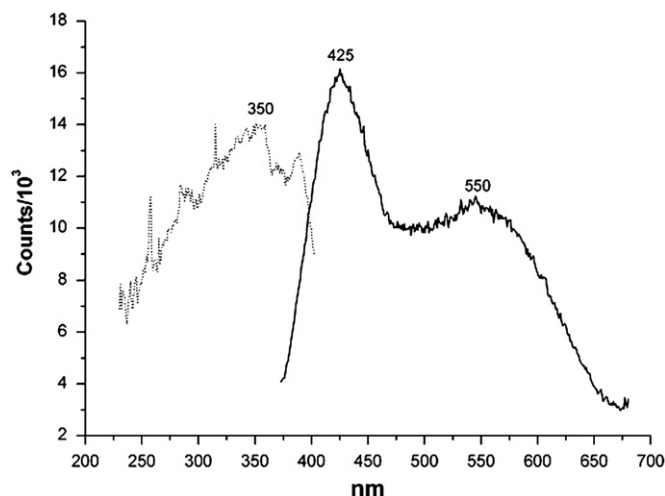


Fig. 9. Solid-state excitation (dashed curves) and emission (solid curves) spectra for compound **2**.

380 °C, and the second step is from 380 to 700 °C. The two steps partially overlapped, corresponding to the condensation of the hydroxyl groups in both the phosphonate ligands and the removal of organic moieties ($\text{CH}_2\text{-Ph-CH}_2$) of *trans*- H_2BDPP . The observed mass loss of two steps of 16.5% is consistent with the calculated value (15.9%) (Fig. S8).

Compound **2** has a 3-D framework with no water molecules, so it can stable up to 330 °C. Two steps of main mass losses (Fig. S9) were observed which corresponds to the condensation of the hydroxyl groups of *trans*- H_2BDPP and the removal of organic moieties ($\text{CH}_2\text{-Ph-CH}_2$) of *trans*- H_2BDPP . The observed mass loss of two steps of 22.5% until to 550 °C, which is close the calculated value (21.91%).

4. Conclusions

In summary, two cadmium phosphonate coordination polymers $[\text{Cd}(\text{cis-}\text{H}_4\text{BDPP})(2,2'\text{-bipy})_2] \cdot (\text{trans-}\text{H}_2\text{BDPP})$ (**1**) and $\text{Cd}(\text{trans-}\text{H}_2\text{BDPP})(\text{phen})$ (**2**) were successfully synthesized under hydrothermal conditions. The *p*-xylenediphosphonic acid is found to be excellent precursor for constructing different kinds of structure motifs, such as 1D chain in **1** and 3D architecture in **2**. There are two different configurations of *p*-xylenediphosphonic acid, *trans*- and *cis*-configurations. The coordinated *cis*-configuration in compound **1** is first found in cadmium *p*-xylenediphosphonate. The choice of the second ligand influences the reaction and the crystal structure of the final products. Compounds **1** and **2** were the first examples of the inorganic–organic hybrid materials, constructed from cadmium paraxlylenediphosphonate and second organic ligand. The results revealed that the coordination mode of the organic diphosphonic acid and the auxiliary N-donor ligands play an important role in the formation of coordination frameworks and would further mediate their optical properties. It is believed that the preliminary results presented in this paper provide a new way to design new types of diphosphonate complexes with novel crystal structures.

Acknowledgments

This research work was supported by National Natural Science Foundation of China (No. 21003020), Doctoral Fund of Ministry of Education of China (Grant no. 20093514120002), Program for New Century Excellent Talents of Fujian Province (Grant SXSJRC2007-21),

and Science & Technology Promotion Foundation of Fuzhou University (Grant 2009-XY-4).

Appendix A. Supplementary Information

Supplementary data associated with this article can be found in the online version at doi:10.1016/j.jssc.2011.11.043.

References

- [1] (a) X. Shi, G.S. Zhu, S.L. Qiu, K.L. Huang, J.H. Yu, R.R. Angew. Chem. Int. Ed. 43 (2004) 6482;
 (b) A. Distler, S.C. Sevov, Chem. Commun. (1998) 959;
 (c) G.K.H. Shimizu, R. Vaidyanathan, J.M. Taylor, Chem. Soc. Rev. 38 (2009) 1430;
 (d) M. Plabst, L.B. McCusker, T. Bein, J. Am. Chem. Soc. 131 (2009) 18112.
- [2] (a) G.A. Neff, M.R. Helfrich, M.C. Clifton, C.J. Page, Chem. Mater. 12 (2000) 2363;
 (b) T.Y. Ma, X.Z. Lin, Z.Y. Yuan, Chem. Eur. J. 16 (2010) 8487;
 (c) Y.Q. Guo, B.P. Yang, J.L. Song, J.G. Mao, Cryst. Growth Des. 8 (2008) 600;
 (d) S.F. Tang, J.L. Song, X.L. Li, J.G. Mao, Cryst. Growth Des. 6 (2006) 2322.
- [3] (a) Q.M. Gao, N. Guillou, M. Nogues, A.K. Cheetham, G. Ferey, Chem. Mater. 11 (1999) 2937;
 (b) C. Serre, J.A. Groves, P. Lightfoot, A.M.Z. Slawin, P.A. Wright, N. Stock, T. Bein, M. Haouas, F. Taulelle, G. Ferey, Chem. Mater. 18 (2006) 1451;
 (c) P.O. Adelani, T.E. Albrecht-Schmitt, Inorg. Chem. 48 (2009) 2732;
 (d) X.G. Liu, K. Zhou, J. Dong, C.J. Zhu, S.S. Bao, L.M. Zheng, Inorg. Chem. 48 (2009) 1901.
- [4] (a) E. Kuliszewska, M. Hanbauer, F. Hammerschmidt, Chem. Eur. J. 14 (2008) 8603;
 (b) J.L. Song, F.Y. Yi, J.G. Mao, Cryst. Growth Des. 9 (2009) 3273;
 (c) M.J. Bloemink, J.J.H. Diederik, J.P. Dorenbos, R.J. Heetebrij, B.K. Keppler, J. Reedijk, Eur. J. Inorg. Chem. (1999) 1655;
 (d) E.V. Bakhmutova-Albert, N. Bestaoui, V.I. Bakhmutov, A. Clearfield, A.V. Rodriguez, R. Llavona, Inorg. Chem. 43 (2004) 1264.
- [5] (a) J.G. Mao, Z.K. Wang, A. Clearfield, Inorg. Chem. 41 (2002) 3713;
 (b) H.L. Ngo, W.B. Lin, J. Am. Chem. Soc. 124 (2002) 14298;
 (c) J.G. Mao, Z.K. Wang, A. Clearfield, New. J. Chem. 26 (2002) 1010.
- [6] (a) T.B. Liao, Y. Ling, Z.X. Chen, Y.M. Zhou, L.H. Weng, Chem. Commun. 46 (2010) 1100;
 (b) Z. Chen, Y. Zhou, L. Weng, C. Yuan, D. Zhao, Chem. Asian J. 2 (2007) 1549;
 (c) D.K. Cao, S.Z. Hou, Y.Z. Li, L.M. Zheng, Cryst. Growth Des. 9 (2009) 4445.
- [7] X.M. Zhang, Eur. J. Inorg. Chem. (2004) 544.
- [8] T.H. Yang, D.F. Cao, Y.Z. Li, L.M. Zheng, J. Solid. State. Chem. 183 (2010) 1159;
 (b) C.P. Tsao, C.Y. Sheu, N. N. K.H. Lii, Inorg. Chem. 45 (2006) 6361;
 (c) J.L. Song, J.G. Mao, Chem. Eur. J. 11 (2005) 1417.
- [9] (a) E.K. Brechin, R.A. Coxall, A. Parkin, S. Parsons, P.A. Tasker, R.E.P. Winpenny Angew. Chem. Int. Ed. 40 (2001) 2700;
 (b) X.F. Li, Z.L. Xie, J.X. Lin, R. Cao, J. Solid State Chem. 182 (2009) 2290;
 (c) M. Wang, C.B. Ma, D.Q. Yuan, H.S. Wang, C.N. Chen, Q.T. Liu, Inorg. Chem. 47 (2008) 5580.
- [10] (a) V. Chandrasekhar, T. Senapati, E.C. Sanudo, R. Clerac, Inorg. Chem. 48 (2009) 6192;
 (b) B.P. Yang, J.G. Mao, Inorg. Chem. 44 (2005) 566;
 (c) GYucesan, Ming Hui Yu, W. Ouellette, C.J. O'Connor, J. Zubieta, Cryst EngComm. 7 (2005) 480.
- [11] (a) J.L. Song, H.H. Zhao, J.G. Mao, K.R. Dunbar, Chem. Mater. 16 (2004) 1884;
 (b) X.F. Du, S.M. Ying, J.G. Mao, J. Mol. Struct. 788 (2006) 218.
- [12] (a) D.M. Poojary, B.L. Zhang, A. Clearfield, Chem. Mater. 11 (1999) 421;
 (b) F. Fredoueil, D. Massiot, P. Janvier, F. Gingl, M. Bujoli-Doeuff, M. Evain, A. Clearfield, B. Bujoli, Inorg. Chem. 38 (1999) 1831;
 (c) F. Fredoueil, M. Evain, M. Bujoli-Doeuff, B. Bujoli, Eur. J. Inorg. Chem. (1999) 1077.
- [13] N. Stock, T. Bein, J. Solid State Chem. 167 (2002) 330.
- [14] N. Stock, N. Guillou, T. Bein, G. Ferey, Solid State Sci. 5 (2003) 629.
- [15] F.N. Shi, T. Trindade, J. Rocha, F.A.A. Paz, Cryst. Growth Des. 8 (2008) 3917.
- [16] E. Irran, T. Bein, N. Stock, J. Solid State Chem. 173 (2003) 293.
- [17] X.Z. Xu, P. Wang, R. Hao, M. Gan, F.X. Sun, G.S. Zhu, Solid State Sci. 11 (2009) 68.
- [18] (a) J. Hu, H.H. Zhang, Y.N. Cao, C.G. Zhang, S.A. Zhang, Y.P. Chen, R.Q. Sun, Chin. J. Struct. Chem. 28 (2009) 939;
 (b) S. Jones, H.X. Liu, K. Schmidtke, C.C. O'Connor, J. Zubieta, Inorg. Chem. Commun. 13 (2010) 298;
 (c) B.K. Tripurmallu, R. Kishore, S.K. Das, Polyhedron 29 (2010) 2985.
- [19] N.A. Caplan, C.I. Pogson, D.J. Hayes, G.M. Blackburn, J. Chem. Soc. Perkin Trans. 1 (2000) 421–437.
- [20] (a) Sheldrick, SHELXL-97, Program for X-ray Crystal Structure Refinement, University of Gottingen, Gottingen, Germany, 1997;
 (b) G.M. Sheldrick, SHELXS-97, Program for X-ray Crystal Structure Solution, University of Gottingen, Gottingen, Germany, 1997.
- [21] (a) L.Y. Zhang, J.P. Zhang, Y.Y. Lin, X.M. Chen, Cryst. Growth. Des. 6 (2006) 1684;
 (b) J.M. Rueff, S. Pillet, N. Claiser, G. Bonaventure, M. Souhassou, P. Rabu, Eur. J. Inorg. Chem. (2002) 895.